Rhodium-rhodium interactions in [Rh(β-diketonato)$(CO)_2$] complexes

Marrigje Marianne Conradie[a], Petrus.H.van Rooyen,[b] Carla Pretorius,[a] Andreas Roodt [a,]* and Jeanet Conradie[a,]*

[a] Department of Chemistry, PO Box 339, University of the Free State, 9300 Bloemfontein, Republic of South Africa.

[b] Department of Chemistry, University of Pretoria, Private Bag X20, Hatfield, 0028, South Africa.

*Contact author details:

Name: Jeanet Conradie

Tel: +27-51-4012194

Fax: +27-51-4017295

e-mail: conradj@ufs.ac.za

Keywords

Rhodium; β-Diketone; Structure; DFT; dicarbonyl; metal-metal interaction

Graphical abstract

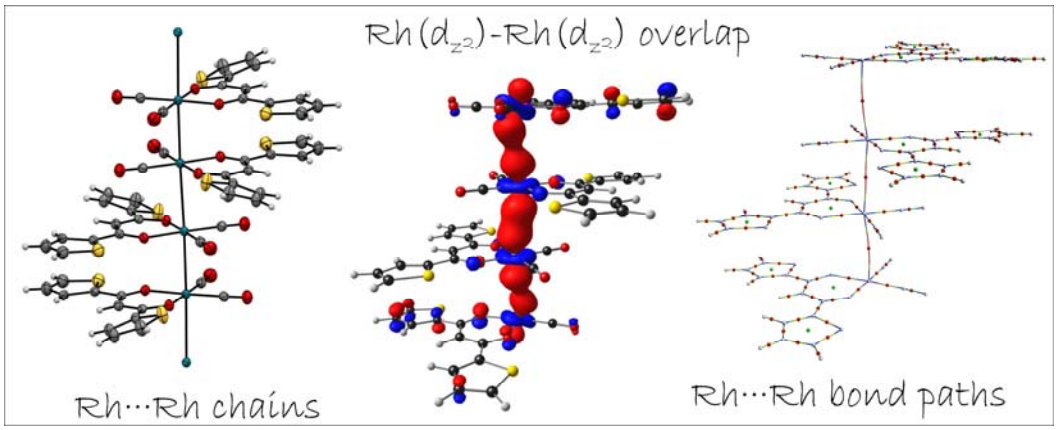

Synopsis

Solid state crystal structure and DFT study of the metallophilic rhodium-rhodium interactions of [Rh(R_1COCHCOR_2)(CO)$_2$] (where R_1, R_2 = CF_3, C_4H_3S or Ph)

Highlights

Crystal structures of [Rh(R_1COCHCOR_2)(CO)$_2$], where R_1, R_2 = CF_3, C_4H_3S or Ph

Metallophilic rhodium-rhodium interactions in the solid state

Sigma-sigma interaction of d_{z2} molecular orbitals

AIM bonding paths

NBO LP(Rh d_{z2})-LP*(Rh p_z) interaction

Abstract

The solid state single crystal structures of [Rh(β-diketonato)(CO)$_2$], where β-diketonato = (R_1COCHCOR_2)$^-$, with R_1, R_2 = CF_3, C_4H_3S (**1**), C_4H_3S, C_4H_3S (**2**), Ph, C_4H_3S (**3**) and CF_3, Ph (**4**), show that these complexes in some cases form dinuclear units, which stack in chains with weak metallophilic rhodium-rhodium interactions, while in other cases they produce continuous polymeric units, with equal intermolecular Rh···Rh distances. Different solid state structural data is reported herein for these four complexes, including a low temperature comparison with ambient data for (**4**). In the latter case, weak intermolecular halogen bonding has also been identified, which additionally contributes to the stability of (**4**) in the solid state. Computational evaluation of the frontier molecular orbitals of both dinuclear and tetranuclear models of complexes (**1**) - (**4**), show Rh(d_{z2})-Rh(d_{z2}) σ bonding and σ* anti-bonding orbitals. An NBO analysis of the dinuclear units, revealed a donor-acceptor interaction between the two rhodium atoms in such a unit, while a QTAIM study identified a bonding path between the two rhodium atoms therein.

1 Introduction

The study of molecules that form one-dimensional chains have long been of interest in physics, as well as in organic, inorganic and organometallic chemistry, because of their magnetic [1], photophysical [2], catalytic [3], semiconductive and conductive [4] properties. The one-dimensional wires have potential applications in for example, light-emitting diodes, photovoltaic cells and molecular sensors [5]. One important class of inorganic complexes, which can form such a one-dimensional wired assembly, is that of square planar transition metal complexes. In the solid state,

stacking within these complexes allows for intermolecular interaction between the molecules through metal-metal and metal-ligand interactions. The formation of metal chains is therefore possible [6,7,8], as illustrated in Scheme 1 (a). It has been shown that square planar rhodium(I) complexes of the type [Rh(β-diketonato)$(CO)_2$] generally form dimer-like arrangements in the solid state, with an intermolecular distance between the metals in the dinuclear unit, ranging from 3.18 to 3.54 Å. Some of these dinuclear units further stack in infinite chains, leading to the formation of stable molecular wires [9,10], see Scheme 1 (b) for β-diketonato = $(CH_3COCHCOCH_3)^-$ (acac). In this contribution, we present the solid state single crystal structures of two [Rh(β-diketonato)$(CO)_2$] complexes, where β-diketonato = $(RCOCHCOC_4H_3S)^-$ and R = CF_3 (**1**) and C_4H_3S (**2**), and compare them to the related complex from literature, where R = Ph (**3**) [9], see Scheme 2. We also present the low temperature single crystal structure of a closely related complex [Rh($CF_3COCHCOC_6H_5$)$(CO)_2$] (**4**), of which the room temperature data is known [11], in order to briefly note what changes temperature might induce in the observed Rh···Rh metallophilic interactions. The data from the solid state studies were subsequently used to initiate a computational chemistry study, wherein the monomers, dinuclear and tetranuclear entities were optimized, of which the results are described in this report.

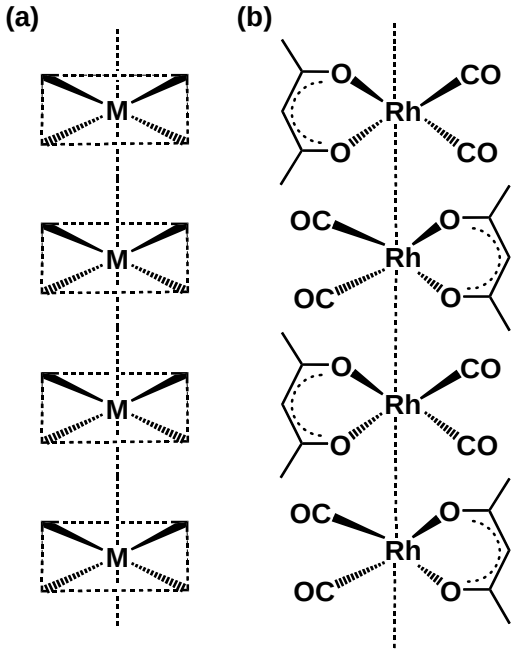

Scheme 1. Stacking in the solid state of (a) square planar transition metal complexes and (b) [Rh($CH_3COCHCOCH_3$)$(CO)_2$], which leads to weak intermolecular metal-metal interactions.

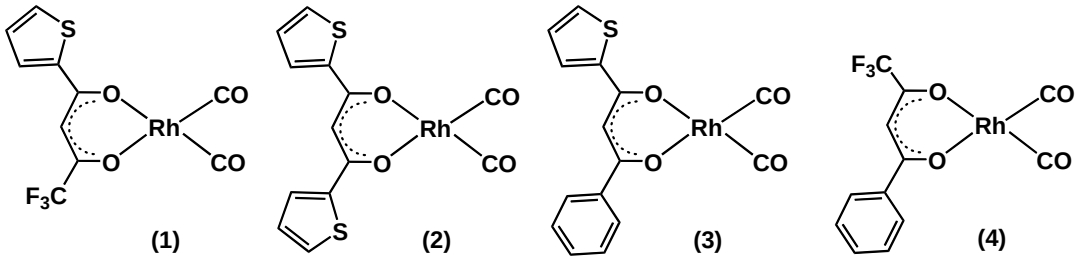

Scheme 2. The [Rh(β-diketonato)$(CO)_2$] complexes investigated in this study; where β-diketone is: Htta = 4,4,4-Trifluoro-1-(2-thienyl)-1,3-butanedione (**1**), Hdtm = 1,3-di(2-thenoyl)-1,3-propanedione (**2**), Hbth = 1-phenyl-3-(2-thenoyl)-1,3-propanedione (**3**) and Htfba = 1,1,1-trifluoro-4-phenyl-2,4-butanedione (**4**).

2 Experimental

2.1 Synthesis

Three complexes [Rh(R_1COCHCOR_2)$(CO)_2$], with R_1 = C_4H_3S, and R_2 = CF_3 (**1**) or C_4H_3S (**2**), as well as R_1 = CF_3, R_2 = Ph (**4**), were synthesized as described previously [12], from $RhCl_3.nH_2O$ [13] and the respective β-diketone [14]. The characterization data of these complexes is provided in the Supporting Information.

2.2 Crystal structure analysis

Data for crystals **1** and **2**, obtained from solutions in hexane, were collected on a Bruker D8 Venture kappa geometry diffractometer, with duo Iμs sources, a Photon 100 CMOS detector and APEX II control software [15], using Quazar multi-layer optics monochromated, Mo-*K*α radiation, by means of a combination of ϕ and ω scans. Data reduction was performed using SAINT + [15] and the intensities were corrected for absorption using SADABS [15]. The structures were solved by intrinsic phasing using SHELXTS and refined by full-matrix least squares, using SHELXTL + [16] and SHELXL-2013+ [16]. The reflection data for **4** was collected on a Bruker X8 Apex II 4K Kappa CCD diffractometer, using graphite monochromated Mo Kα radiation (λ= 0.70926 Å), with ω- and φ-scans at 100(2) K. The Apex II software package [15] was utilised as mentioned above, while refinement was performed using the WinGX software package [17], which incorporates SHELXL [16]. In the structure refinement, all hydrogen atoms were added in calculated positions and treated as riding on the atom to which they are attached. All non-hydrogen atoms were refined with anisotropic displacement parameters. In **1** and **2**, all isotropic displacement parameters for hydrogen atoms were calculated as X × Ueq of the atom to which they are attached, where X = 1.5 for the methyl hydrogens and X = 1.2 for all other hydrogens. In **4**, the hydrogen atoms were

positioned geometrically and refined, utilizing a riding model with fixed C-H distances of 0.95 Å (CH) [U_{iso}(H)= 1.2 Ueq] for aromatic hydrogens, and methyl H-atoms fixed at 0.98 Å (CH) [U_{iso}(H)= 1.2 Ueq]. Crystal data, data collection, structure solution and refinement details are available in the Supplementary Information and in the CIFs (CCDC deposit numbers 1524292 (**1**), 1524293 (**2**) and 1543936 (**4**)).

2.3 Density functional theory (DFT) calculations

Density functional theory (DFT) calculations in this study were performed with the following functionals: PW91 [18], LC-BLYP [19,20,21,22], B3LYP [21,22], CAM-B3LYP [23] (in combination with the Grimme empirical dispersion correction D3 [24]) and M06 [25] (both with and without the D3 correction [26]), as implemented in the Gaussian 09 program package [27]. Geometries of the neutral complexes were optimized in the gas phase with the Lanl2dz basis set for Rh (Los Alamos ECP plus DZ) [28], and 6-311G(d,p) for the other atoms. The natural bond orbital (NBO) calculations were done on the gas phase B3LYP optimized structures, on the same level of theory, using the NBO 3.1 module [29] in Gaussian 09. The topological analysis of the electron charge density, performed for the complexes, was determined using Bader's quantum theory of atoms in molecules (QTAIM) [30], on the gas phase B3LYP optimized structures. The electronic density analysis was performed using QTAIM [31], as implemented in ADF2013 [32], at the same level of theory. The 6-311G(d,p)/Lanl2dz basis set proved to give reliable geometries and energies for rhodium-dicarbonyl complexes containing a β-diketonato ligand [33,34,35].

3 Results and Discussion

3.1 X-ray crystallography

Perspective drawings [36] of the molecular structure of complexes [Rh($CF_3COCHCOC_4H_3S$)$(CO)_2$] (**1**), [Rh($C_4H_3SCOCHCOC_4H_3S$)$(CO)_2$] (**2**) and [Rh($CF_3COCHCOPh$)$(CO)_2$] (**4**), showing the crystallographic numbering scheme used, are presented in Figure 1 (a)-(c). Comparative packing diagrams of (**1**), (**2**) and also of [Rh($PhCOCHCOC_4H_3S$)$(CO)_2$] (**3**) from a previous study, are given in Figure 2 (a)-(c), while that of complex (**4**) is illustrated in Figure 3, together with selected interaction domains as discussed later. Table 1 lists selected geometrical parameters of (**1**) - (**4**), as well as other related [Rh(β-diketonato)$(CO)_2$] complexes obtained from literature that also stack in infinite chains in the solid state, with weak metallophilic rhodium-rhodium interactions.

[Rh($CF_3COCHCOC_4H_3S$)$(CO)_2$] (**1**) crystallised with four crystallograpically independent molecules (two dinuclear pairs) per asymmetric unit. The 2-thienyl group is in a *syn* orientation relative to the O atom of the diketonato moiety, with the S-C-C-O torsion angles being close to 0°**.** No proof for the existence of the *anti* orientation of the thienyl group, relative to the O atom of the diketonato moiety, could be found in the crystal structure of (**1**). The thienyl substituents and the C atoms of the CF_3 groups are all in virtually the same planes as their respective diketonato moieties, resulting in almost completely planar molecules. Two of the four CF_3-groups in the asymmetric unit showed some positional disorder of the fluorine atoms, and the anisotropic parameters were modelled to stabilize the refinement, as described in the CIF file. Significantly close Rh···Rh interactions are observed in (**1)** (namely 3.2311(6) Å and 3.6220(6) Å for dinuclear pair 1, as well as 3.4120(6) and 3.3664(6) for dinuclear pair 2), resulting in packing of the dinuclear pairs in infinite chains, in the direction of the a-axis (Figure 2 a). It is noteworthy that the Rh···Rh distance within dinuclear pair 1 of (**1)** and the Rh···Rh distance within dinuclear pair 2 of (**1)** differ by 0.135 Å, while the respective distances between the separate dinuclear pairs differ by 0.210 Å. The Rh-O and Rh-C bonds differ up to 0.02 Å, when comparing the same bond in the four different molecules per asymmetric unit of complex (**1**), (See Table S3 in the Electronic Supporting Information).

[Rh($C_4H_3SCOCHCOC_4H_3S$)$(CO)_2$] (**2**) crystallised with only one molecule per asymmetric unit, and displayed orientational disorder in the position of the sulfur atoms of the two terminal thienyl substituents. The molecular structure of the major conformation (>90%) has S-C-C-O torsion angles of approximately 0°, while that of the minor conformation (<10%) is approximately 180º. The ratio of the two conformations was refined to 0.920(3) : 0.080(3). The main conformation of complex (**2**) is presented in Figure 1. The angle between the planes of the two 2-thienyl groups is 17° and this indicates that the molecular conformation is slightly less planar than in (**1**). Also significantly close intermolecular Rh···Rh interactions of 3.1903(4) and 3.3174(4) Å, respectively, are observed in (**2).** The dinuclear units therefore stack in infinite chains, with intermolecular Rh···Rh distances within the limits (3.18 to 3.54 Å) observed for [Rh(β-diketonato)$(CO)_2$] complexes [9].

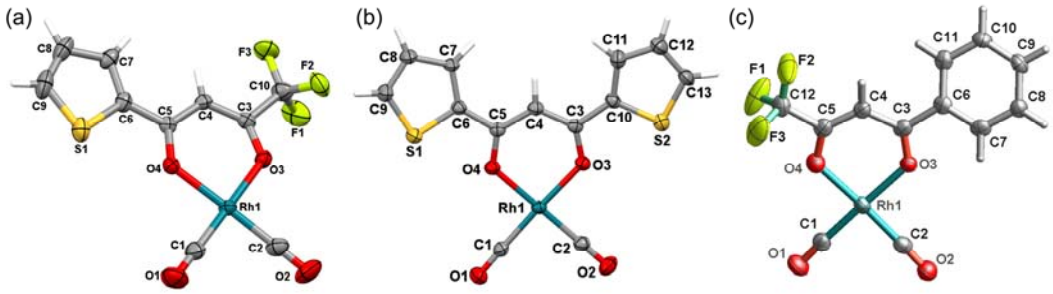

Figure 1. Perspective drawings, showing the atom numbering scheme, of the molecular structure of complexes (**a**) [Rh($CF_3COCHCOC_4H_3S$)$(CO)_2$] (**1**); (**b**) [Rh($C_4H_3SCOCHCOC_4H_3S$)$(CO)_2$] (**2**), disordered over two positions in the ratio 0.920 : 0.080 (major domain shown), and (**c**) [Rh($CF_3COCHCOPh$)$(CO)_2$] (**4**). Atomic displacement parameters (ADPs) are shown at the 50 % probability level.

[Rh($CF_3COCHCOPh$)$(CO)_2$] (**4**) crystallised in the orthorhombic space group *Pbca*, with only one molecule in the asymmetric unit and 8 formula units in the unit cell. This structure represents a low temperature determination of the complex, as published by Leipoldt *et al.* [11] in 1977. The published structure reported a collection at room temperature, however the short communication paper offered very little information with regards to the reliability of the data, as key factors such as completeness of the data collection and Goodness-of-Fit etc. could not be established. Moreover, bond data was very inaccurate, and a re-determination of the structure was therefore undertaken at low temperature.

The unit cell dimensions of the published structure by Leipoldt *et al.* [11] for complex (**4**), are given in the Supplementary Data Table S1, for comparison to the dimensions of the structure determined in this study. No standard deviations have been supplied on the unit cell dimensions of the published structure. The slight deviations observed for the unit cell dimensions, as seen in Supplementary Data Table S1, are attributed to the temperature at which the data collection was performed, with room temperature collections typically resulting in an increase of lattice parameters, since the lattice expands anisotropically with an increase in temperature [37]. Further aspects regarding the temperature variation in the unit cell dimensions, are discussed in more detail below.

It is obvious from Table 1, with more detail given in Supplementary Data Table S2, that the low temperature structure for complex **4** obtained in this study offers significantly more accurate information than the older structure in [11], with regard to the bond distances and angles, as is evident from the large ESD values present on the data for the previously published structure of

[Rh(CF$_3$COCHCOPh)(CO)$_2$] (**4**). This is particularly important when accurate interatomic bond data isrequired, which is necessary for more systematic comparison and identification of observed geometric changes. Large error values are not uncommon for data originating from several decades ago, since the improvement of modern techniques and software in crystallography, has lately led to a reduction in the errors observed for data. In addition, temperature effects could also account for some of the differences observed in the bond lengths and angles between the two structures. Elevated temperatures generally result in larger thermal parameters for atoms, since the movement of atoms is less restricted, leading to an *increase* in reported bond lengths and angles. [38]

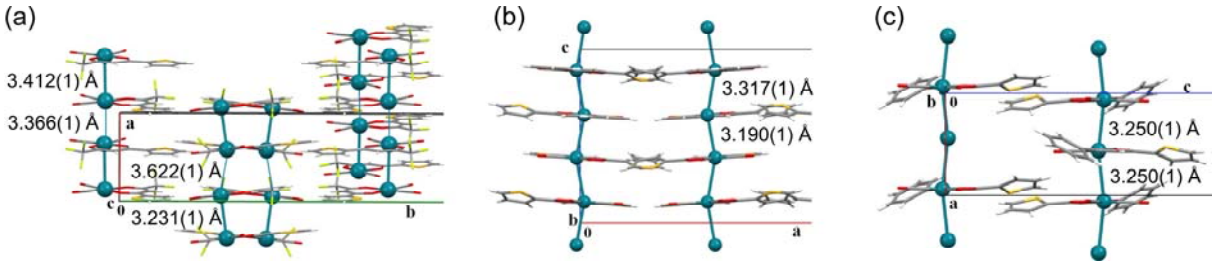

Figure 2. Selected fractions of the unit cells of complexes **1-3**, illustrating the packing diagrams of (**a**) [Rh(CF$_3$COCHCOC$_4$H$_3$S)(CO)$_2$] (**1**), (**b**) [Rh(C$_4$H$_3$SCOCHCOC$_4$H$_3$S)(CO)$_2$] (**2**) and (**c**) [Rh(PhCOCHCOC$_4$H$_3$S)(CO)$_2$] (**3**)**.** The Rh-atoms are drawn as spheres and the Rh···Rh contacts between the dinuclear pairs (see (**a**)) are indicated by thinner lines. Selected Rh···Rh distances are shown.

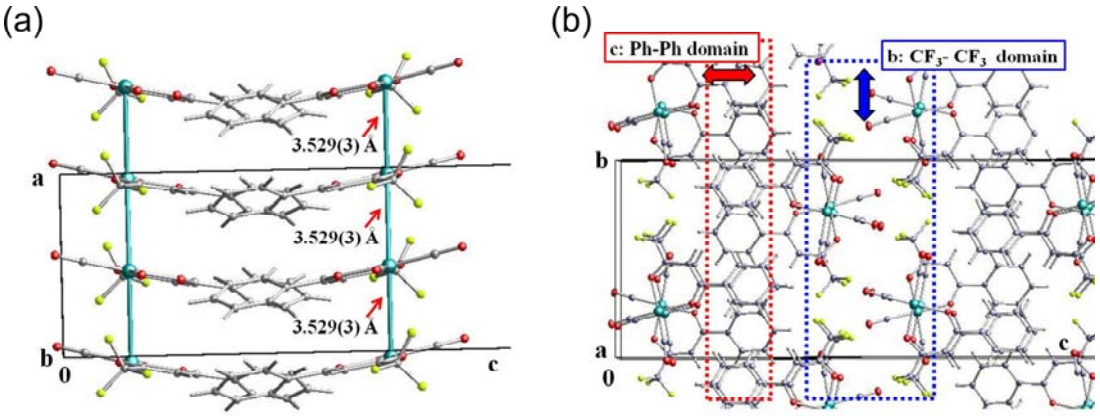

Figure 3. The packing diagram of [Rh(CF$_3$COCHCOPh)(CO)$_2$] (**4**), indicating (**a**) the Rh···Rh interactions along the a-axis (virtually temperature independent), and (**b**) the weaker interaction domains along the b- and c-axes, respectively.

Relative changes, namely a decrease in all three cell axes with decreasing temperature (from 293 K to 100 K) are as follows: *a*=0.17%, *b*=1.3% and *c*=2.9%. Figure 3(b) illustrates that the *b*- and *c*-domains allow for compression. The *c*: Ph-Ph domain, representing weak interactions from primarily the Phenyl rings, also exhibits the largest decrease observed. The *b*-axis on the other

hand, defined along the *b*: CF_3-CF_3 domain, see Figure 4, is clearly not as affected by temperature as the Ph-Ph domain. However, what is quite surprising is that the *a*-axis direction, defined by the Rh···Rh metallophillic interactions, merely decreased by 0.17%. Therefore these Rh···Rh interactions in the *a*-axis direction, at least in this example, do not seem to be affected by temperature as much as the other domains. In fact, the metallophilic bonds merely decrease from 3.537(3) at 293 K, to 3.529(3) Å at 100 K, which implies that the Rh···Rh distances in principle stayed virtually *constant*. This temperature independency could in future be potentially utilised to enable the fabrication of nano-wires and even nanoplates.

The Rh···Rh metallophilic interactions in complex (**4**) are packed along the shortest cell axis (*a*-axis = 7.016(4) Å), similarly to complexes (**1**) and (**3**) above. The Rh···Rh interactions observed in (**4**) however are *ca*. 0.16 Å longer than the Rh···Rh interactions in (**1**) – (**3**) and similar Rh-complexes, see Table 1**.** As noted above, the Rh···Rh interactions lead to the construction of a one-dimensional metal chain, with an angle of 167.50(2)° between consecutive rhodium centres (Rh···Rh···Rh) for (**4**), that compaire well with the Rh···Rh···Rh angle obtained for other [Rh(β-diketonato)$(CO)_2$] complexes that also stack infinite in chains in the solid state (Table 1).

Traditionally, the smaller fluorine atoms have been excluded as potential halogen bond donors, while heavier halogen atoms such as iodine, bromine and chlorine were unequivocally accepted as participating in halogen bonds. This notion was based on the theory that halogen bonds originate through the interactions of a positively charged σ-hole present on a halogen atom with negative sites of nucleophiles [39]. For the heavier halogens, the existence of these σ-holes were undisputed, but only recently has consensus been reached that fluorine may also possess σ-holes, which result in halogen bonding [40]. Halogen bonds are typically encountered along the bond, at angles of approximately 180° between donor and acceptor sites. This holds true, except in cases where secondary interactions are found to disrupt this arrangement [40]. The halogen bonds between molecules of [Rh(CF_3COCHCOPh)$(CO)_2$] (**4**) are illustrated in Figure 4 (a) and data related to the interactions given in the caption. The interactions result in polymeric chains within the crystal lattice along the *b*-axis, resulting in a 3-dimensional connected structure, as illustrated in Figure 4 (b).

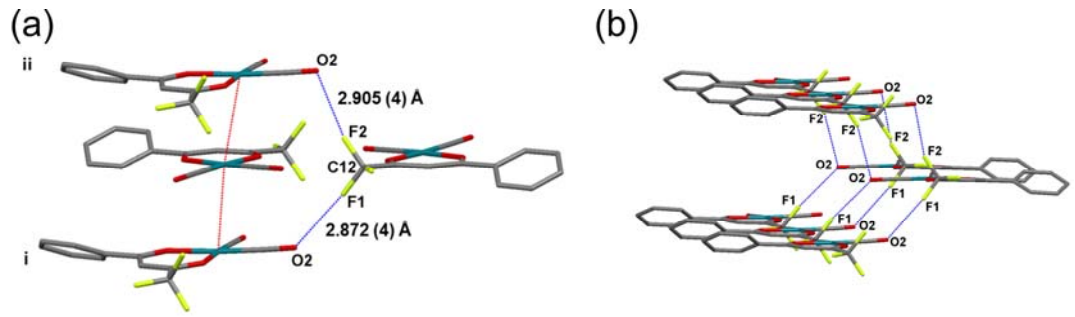

Figure 4. (a) Weak intermolecular C-F···O interactions (indicated in blue) observed for C12-F2···O2^{ii} and C12-F1···O2^{i} in [Rh(CF_3COCHCOPh)$(CO)_2$]. The two significant interactions illustrated in (a) are (i) C12-F1···O2^{i}, 1.315(5), 2.872(4), 4.183(6),174.6°(3); and (ii) C12-F2···O2^{ii}; 1.318(5); 2.905(4); 4.142(6); 155.8°(3), respectively. The symmetry codes are as follows: i) 5/2-x, -1/2+y, -z; ii) 3/2-x, -1/2+y, -z. (b) Intermolecular halogen bonds (indicated in blue) connect neighbouring molecules *via* the carbonyl moeity of [Rh(CF_3COCHCOPh)$(CO)_2$] in a head-to-tail motif, forming a polymeric chain along the *b*-axis. The Halogen bonds are indicated by the following five geometric parameters: D-X···A; dD-X (Å); dX···A (Å); dD···A (Å); Angle D-X···A (°).

The [Rh(β-diketonato)$(CO)_2$] complexes discussed in this study, as well as the complexes listed in Table 1, all either form dinuclear units which stack in infinite chains with weak metallophilic rhodium-rhodium interactions, or they produce continuous polymeric units, with equal Rh···Rh distances. It is also observed that [Rh(β-diketonato)$(CO)_2$] complexes sometimes form dinuclear [Rh(β-diketonato)$(CO)_2]_2$ units that do not form infinite metal-metal chains in the solid state [34,41,42,43].

Table 1. Selected geometric parameters for the indicated [Rh(β-diketonato)$(CO)_2$] complexes, which stack an infinite chain of rhodium atoms (where β-diketonato = $(R_1C3O3C4HC5O4R_2)^-$, with R_1 and R_2 groups as indicated).

R_1 [a]	**R_2** [a]	**Rh–O3 / Å** [a]	**Rh–O4 / Å** [a]	**Rh–C2 / Å** [a]	**Rh–C1 / Å** [a]	**O4–Rh–O3 / °**	**C1–Rh–C2 / °**	**Torsion angle between molecules in dinuclear units / °** [b]	**(Rh···Rh··Rh) / °**	**Rh··Rh / Å**	**CCDC ref code / Reference**
CF_3	C_4H_3S	2.034(4)[c]	2.040(4)[c]	1.846(6)[c]	1.838(6)[c]	90.22(14)[c]	88.8(3)[c]	62	156.32(2)	3.231(1); 3.622(1)[d]	this study (**1**)
								68	163.44(2)	3.366(1); 3.412(1)[d]	this study (**1**)
C_4H_3S	C_4H_3S	2.031(1)	2.037(1)	1.852(2)	1.847(2)	90.44(6)	88.31(8)	43	160.08(1	3.190(1); 3.317(1)	this study[e] (**2**)
CF_3	Ph	2.02(2)	2.02(2)	1.82(3)	1.79(3)	89.8(7)	86.2(2)	114	172.06(3)	3.537	BTFARH [11]
CF_3	Ph	2.030(4)	2.043(3)	1.854(4)	1.832(5)	89.7(1)	87(1)	115	167.50(2)	3.529(3)	this study (**4**)
Ph	C_4H_3S	2.042(6)	2.027(6)	1.846(8)	1.866(9)	90.4(2)	88.1(3)	180	167.38(2)	3.250(1)	TIRZOL [9] (**3**)
CH_3	CH_3	2.040(4)	2.044(4)	1.831(7)	1.831(7)	90.8(2)	88.9(3)	180	175.28	3.253, 3.271	ACABRH02 [44]
Ph	CH_3	2.050(1)	2.035(1)	1.854(2)	1.848(2)	90.61(5)	87.98(7)	180	172.06(1)	3.307(1), 3.460(1)	EDOYAZ [45]

[a] Numbering according to Figure 1. R_1 is attached to C3 and R_2 to C5.

[b] Angle measured as torsion $C_{methineH\text{-}\beta\text{-}diketonato\ ligand\ molecule\ 1} - Rh_{molecule\ 1} - Rh_{molecule\ 2} - C_{methineH\text{-}\beta\text{-}diketonato\ ligand\ molecule\ 2}$

[c] Average values for all 4 molecules

[d] Two dinuclear pairs per asymmetric unit, for complex (**1**), therefore two sets of Rh–Rh interactions

[e] Values for the major domain

3.2 Computational chemistry study

To obtain more information on the Rh···Rh metallophilic interactions observed in the [Rh(β-diketonato)$(CO)_2$] complexes described in this report, a computational chemistry study, utilizing density functional theory, is presented. The mononuclear complex, as well as a dinuclear unit and a tetranuclear model (consisting of two dinuclear units), were all three optimized, using a selection of different types of DFT functionals, namely the pure functional PW91, the Minnesota functional M06 (with and without Grimme empirical dispersion correction D3), the hybrid functional B3LYP, as well as the long range corrected functionals LC-BLYP and CAM-B3LYP (with D3). The dinuclear unit is considered to be the elementary unit of the infinite Rh···Rh chains observed in the [Rh(β-diketonato)$(CO)_2$] crystals. In order to obtain more information on the electronic structure of these dinuclear units, a natural bond orbital (NBO) and atoms in molecules (QTAIM) analysis on the dinuclear units, were also performed.

3.2.1 Structure

The optimized structure of each of the [Rh($R_1COCHCOR_2$)$(CO)_2$] complexes, with R_1, R_2 = CF_3, C_4H_3S (**1**), C_4H_3S, C_4H_3S (**2**), Ph, C_4H_3S (**3**) or CF_3, Ph (**4**), showed the expected square planar geometry around rhodium for each mononuclear [Rh(β-diketonato)$(CO)_2$] unit, see Supplementary Data Table S3 for selected bond lengths and angles, obtained by the different functionals. The most important bond lengths and angles in these [Rh(β-diketonato)$(CO)_2$] complexes, are considered those involving rhodium. The optimized Rh-ligand bond lengths in the mononuclear units, although slightly overestimated, compare well with the single crystal X-ray structure values, up to 0.05 Å for Rh-O bond lengths and up to 0.03 Å for Rh-C bond lengths, depending on the functional used. Slightly larger DFT calculated bond lengths than experimental solid state data are generally observed for gas phase optimizations [46], and gas phase optimizations of related rhodium-β-diketonato complexes [34,35,47]. Differences between experimentally measured metal-ligand bond lengths and calculated bond lengths below a threshold of 0.02 Å, are considered as meaningless [46]. Results obtained when applying the PW91, LC-BLYP and CAM-B3LYP functionals, compared the best with experimental data, exhibiting deviations from experimental data comparable to the small differences in the experimentally measured Rh-O bond lengths (of 0.021 Å) and Rh-C bond lengths (of 0.016 Å), of the four molecules of complex (**1**), for the two dinuclear pairs per asymmetric unit.

The DFT optimized Rh···Rh distances within a dinuclear unit, as well as the Rh···Rh distances between two different dinuclear units (tetranuclear model), are given in Table 2 for (**1**) – (**4**). Generally the PW91, M06 and LC-BLYP functionals gave better agreement with the experimental values (obtained from solid state crystal data) than B3LYP and CAM-B3LYP. The intermolecular Rh···Rh distances within a dinuclear unit, optimized either as a dinuclear unit or in the tetranuclear model, did not change significantly and agree within 0.22 Å with the experimental measurements, when applying the PW91, M06 and LC-BLYP functionals. Since the experimentally measured intermolecular Rh···Rh distances in the two different dinuclear units of complex (**1**) vary by 0.14 Å, the differences between experimental and calculated values for (**1**) – (**4**), as obtained by the PW91, M06 and LC-BLYP functionals, are not considered to be significant.

The experimentally measured Rh···Rh distances between the two dinuclear pairs per asymmetric unit of complex (**1**), are 3.622 Å for dinuclear pair 1, and 3.412 Å for dinuclear pair 2, see Figure 2 (a). These experimental Rh···Rh distances between dinuclear units differ by 0.21 Å. Therefore the DFT calculated Rh···Rh distance between dinuclear units for (**1**) – (**4**), as obtained by PW91, M06 and LC-BLYP, compares well with experiment (within 0.22 Å for PW91, 0.20 Å for M06 and 0.11 Å for LC-BLYP) and is comparable to the related experimental 0.21 Å difference for complex (**1**).

Table 2. Selected experimental and DFT calculated Rh···Rh distances (Å) for (**1**) - (**4**), optimized as both dinuclear or tetranuclear models, using the indicated functionals.

Optimized as dinuclear model		experimental	B3LYP	PW91	M06	M03-D3	LC-BLYP	CAM-B3LYP-D3
1	Rh···Rh in dinuclear unit	3.366; 3.231[a]	3.642	3.310	3.246	3.267	3.403	3.388
2	Rh···Rh in dinuclear unit	3.190	3.648	3.332	3.243	3.249	3.388	3.441
3	Rh···Rh in dinuclear unit	3.250	3.527	3.250	3.148	3.187	3.189	3.946
4	Rh···Rh in dinuclear unit	3.529	3.715	3.306	3.390	3.547	3.518	3.604
Optimized as tetranuclear model		experimental	B3LYP	PW91	M06	M03-D3	LC-BLYP	CAM-B3LYP-D3
1	Rh···Rh in dinuclear unit	3.366; 3.231 [a]	3.668	3.319	3.249	3.254	3.545	3.435
	Rh···Rh in dinuclear unit		3.666	3.320	3.243	3.249	3.548	3.441
	Rh···Rh between dinuclear units	3.412; 3.622	3.696	3.324	3.264	3.236	3.427	3.394
2	Rh···Rh in dinuclear unit 1	3.190	3.732	3.346	3.258	3.258	3.411	3.439
	Rh···Rh in dinuclear unit 2		3.732	3.346	3.248	3.258	3.411	3.439
	Rh···Rh between dinuclear units	3.317	3.593	3.301	3.179	3.183	3.206	3.198
3	Rh···Rh in dinuclear unit 1	3.250	3.607	3.290	3.171	3.342	3.206	3.960
	Rh···Rh in dinuclear unit 2		3.627	3.293	3.176	3.497	3.207	4.209
	Rh···Rh between dinuclear units	3.250	3.600	3.328	3.184	3.180	3.234	4.144
4	Rh···Rh in dinuclear unit 1	3.529	3.730	3.321	3.344	3.350	3.576	3.638
	Rh···Rh in dinuclear unit 2		3.730	3.313	3.306	3.748	3.481	3.802
	Rh···Rh between dinuclear units	3.529	3.719	3.301	3.733	3.292	3.567	3.535

[a] two different dinuclear units within one unit cell

3.2.2 Molecular orbitals

The d^8 [Rh(RCOCHCOC$_4$H$_3$S)(CO)$_2$] complexes (**1**) - (**3**) as well as the related complex (**4**), have a *d* electron configuration of $d_{xz}{}^2 d_{yz}{}^2 d_{xy}{}^2 d_{z^2}{}^2 d_{x^2-y^2}{}^0$, with the HOMO (highest occupied molecular orbital) a nonbonding orbital of mainly d_{z^2} character [10]. The d_{z^2} HOMO is available to form σ bonding and σ* antibonding MOs between two rhodium centres, leading to stacking of complexes (**1**) - (**4**) in the solid state, with σ and σ* Rh(d_{z2})-Rh(d_{z2}) interactions. The frontier MOs involved in the d_{z2} bonding and antibonding of (**1**) - (**4**), are illustrated in Figure 5. The HOMOs of both the dinuclear and tetranuclear models show the antibonding interaction between d_{z2} MOs on rhodium. Figure 5 shows that mainly three MOs are involved in σ Rh(d_{z2})-Rh(d_{z2}) bonding interactions, namely: (i) a MO with σ Rh(d_{z2})-Rh(d_{z2}) bonding interactions within the dinuclear units, (ii) σ Rh(d_{z2})-Rh(d_{z2}) bonding interactions between the dinuclear units in the tetramer, and (iii) a MO with σ Rh(d_{z2})-Rh(d_{z2}) bonding interactions between all Rh centres. Similar σ Rh(d_{z2})-Rh(d_{z2}) bonding MOs are observed for all four complexes (**1**) - (**4**), irrespective of the relative orientation between the two molecules within a dinuclear unit (namely 62° or 68° (for the two dinuclear units in a unit cell of complex **1**), 43°, 180° and 114° for (**1**) - (**4**) respectively), or the relative orientation of the dinuclear units to each other (0°, 180°, 0° and 0° for (**1**) - (**4**) respectively), as illustrated in Figure 6.

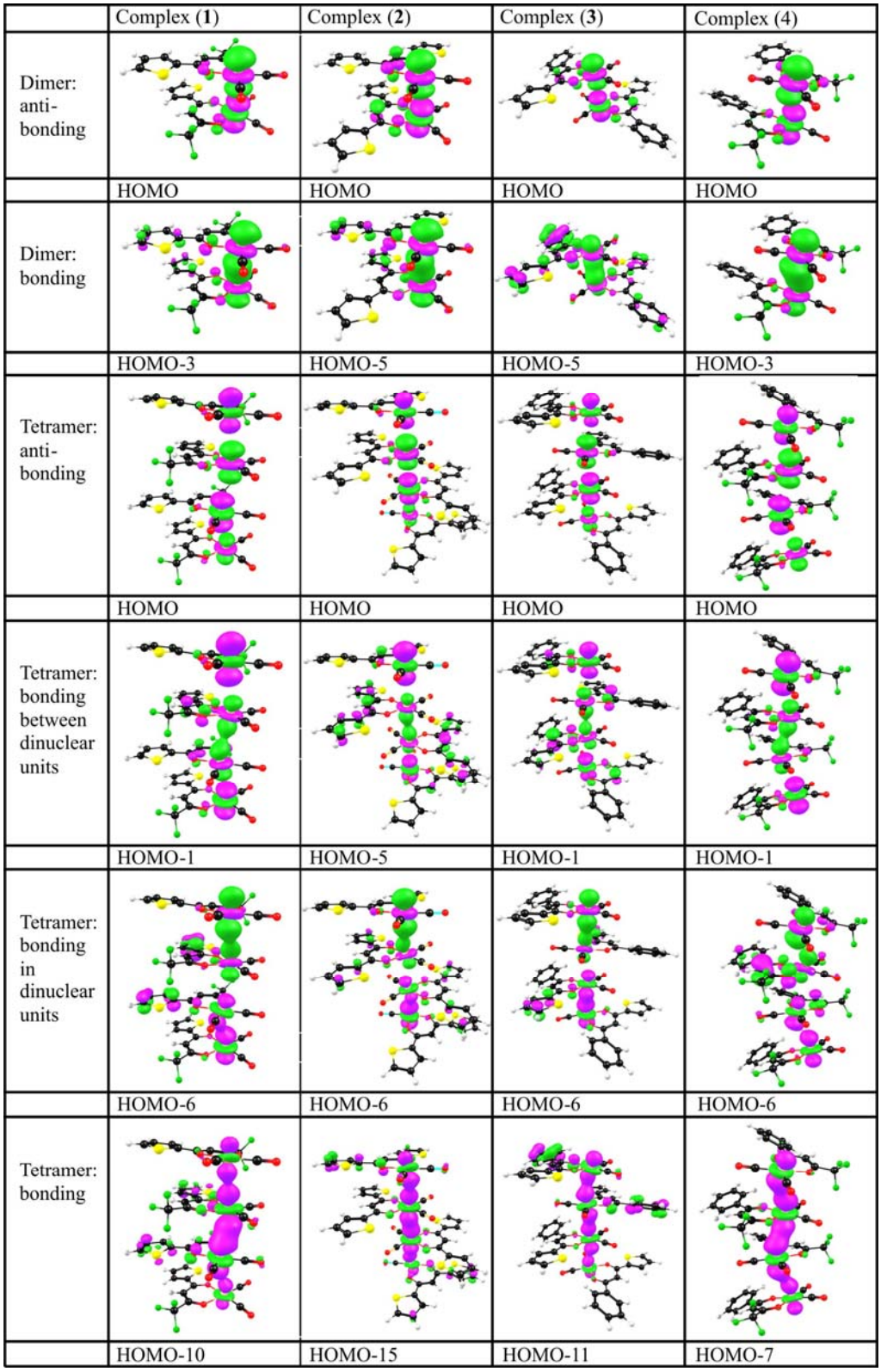

Figure 5. Selected molecular orbitals of the optimized structure of the [[Rh(R_1COCHCOR_2)(CO)$_2$] complexes, with R_1, R_2 = CF_3, C_4H_3S (**1**), C_4H_3S, C_4H_3S (**2**), Ph, C_4H_3S (**3**) and CF_3, Ph (**4**), optimized as either dinuclear or tetranuclear model. Colour code of atoms (online version): Rh (pink), S (yellow), F (green), C (black), O (red), H (white).

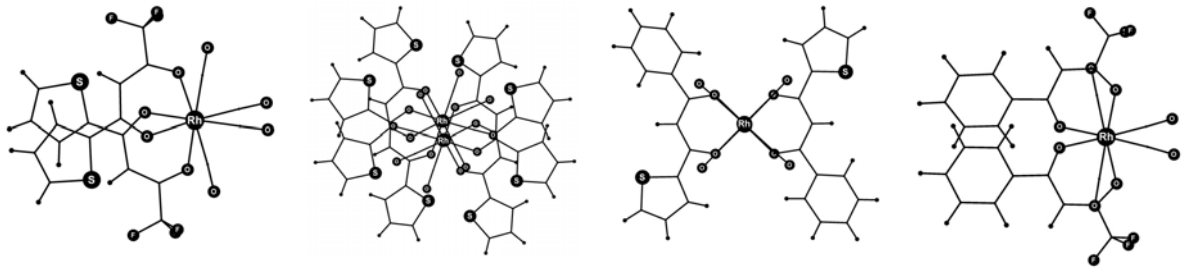

(**1**) (**2**) (**3**) (**4**)

Figure 6. Relative orientation of the two molecules within a dinuclear unit, as well as the dinuclear units to each other (the dinuclear units are overlapping for (**1**), (**3**) and (**4**) and rotated by 180° for (**2**)).

3.2.3 NBO

Evaluation of the results of the natural bond orbitals analyses of the dinuclear rhodium units, revealed a direct intermolecular Rh···Rh interaction between a NBO LP(Rh d_{z2}) of high occupancy of *ca*. 1.97 on Rh of one unit, to a NBO LP*(Rh p_z) of low occupancy of *ca*. 0.06 on Rh of the other unit. See Figure 7 for a visualization of this interaction for complexes (**1**) - (**3**). The NBO interaction energy, E(2), as calculated by the "Second Order Perturbation Theory Analysis of Fock Matrix in NBO Basis", is given in **Table 3**. Complex (**3**) with the two molecular units orientated 180° relative to each other, showed the strongest NBO interaction energy, of over 4 kcal/mol. No NBO donor-acceptor interaction involving the two Rh atoms was observed in (**4**). This result agrees with the longer experimentally measured Rh···Rh intermolecular distance for (**4**), relative to that of (**1**) – (**3**), see Table 1**.**

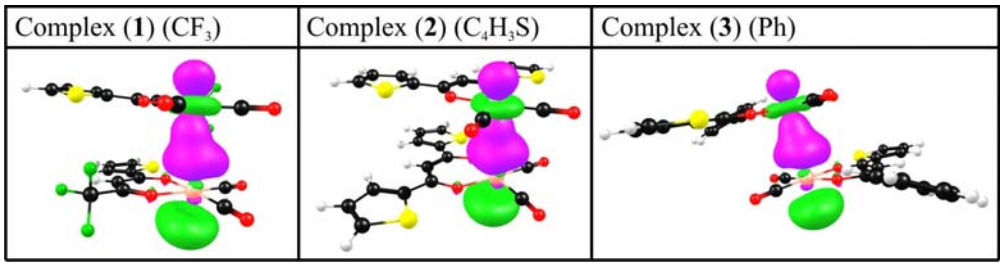

Figure 7. NBO LP(Rh d_{z2}) to LP*(Rh p_z) donor-acceptor interaction in the gas phase DFT optimized structure for $[Rh(RCOCHCOC_4H_3S)(CO)_2]_2$, with R = CF_3 (**1**), C_4H_3S (**2**) and Ph (**3**). The NBO plots use a contour of 60 e/nm^3. Colour code of atoms (online version): Rh (pink), S (yellow), C (black), O (red), H (white).

Table 3. NBO type, occupancies and interaction energies, E(2), as calculated for dinuclear units of (**1**) – (**3**). The two rhodium atoms within the dinuclear unit are numbered Rh1 and Rh2 in the table.

Com-plex	Donor NBO	Acceptor NBO	E(2)	Rh···Rh distance

	type	occupancy	type	occupancy	kcal/mol	Å
1	LP(Rh1 d_{z2})	1.969	LP*(Rh2 p_z)	0.055	2.98	3.642
	LP(Rh2 d_{z2})	1.969	LP*(Rh1 p_z)	0.055	2.98	
2	LP(Rh1 d_{z2})	1.969	LP*(Rh2 p_z)	0.059	3.14	3.648
	LP(Rh2 d_{z2})	1.969	LP*(Rh1 p_z)	0.059	3.14	
3	LP(Rh1 d_{z2})	1.965	LP*(Rh2 p_z)	0.063	4.26	3.527
	LP(Rh2 d_{z2})	1.966	LP*(Rh1 p_z)	0.063	4.13	

3.2.4 QTAIM

A quantum theory of atoms in molecules (QTAIM) analysis of the dinuclear units of complexes (**1**) – (**4**), identified a bond critical point (BCP) and a bond path between the two rhodium atoms within a dinuclear unit of all four [Rh(R_1COCHCOR_2)(CO)$_2$] complexes (**1**) – (**4**), see Figure 8. The existence of such a bond path and its associated bond critical points (BCPs) is sufficient to establish a bonding interaction [48]. In addition, complex (**1**) has two intermolecular bond paths between the S of the thienyl group of one molecule and an F of the CF_3 group of a different molecule. Complex (**3**) has, in addition to the bond path between the two rhodium atoms, also two H···H intra- and one O···H intermolecular bond path. Complex (**4**) has, in addition to the bond path between the two rhodium atoms, two H···H intramolecular bond paths. Data associated with selected intra- and inter-molecular bond paths identified for (**1**) – (**4**), are summarized in **Table 4**. The identified intermolecular bond paths between adjacent molecules in dinuclear units, lead to stabilisation of the stacking of (**1**) – (**4**) in linear chains along the Rh-Rh axis.

Table 4. QTAIM results for the bond critical points (BCP) of the intra- and inter-molecular bond paths (BP) in dinuclear units of (**1**) – (**4**). The BCP numbers are as shown in Figure 8.

Dinuclear units of complex	CP no	Bond path type	inter-atomic distance / Å	Electron density ρ / e a_0^{-3}	Laplacian of electron density $\nabla^2\rho$ / e a_0^{-5}
(**1**)	1	Rh···Rh	3.642	0.0092	0.0203
	2	S···F	3.870	0.0019	0.0073
	3	S···F	3.865	0.0019	0.0072
(**2**)	4	Rh···Rh	3.648	0.0093	0.0202
(**3**)	5	Rh···Rh	3.527	0.0117	0.0255
	6	O·· H	3.209	0.0020	0.0081
	7	H···H	2.114	0.0122	0.0494
	8	H···H	2.106	0.0123	0.0495
(**4**)	9	Rh···Rh	3.715	0.0078	0.0174
	10	H···H	2.100	0.0122	0.0496
	11	H···H	2.048	0.0128	0.0501

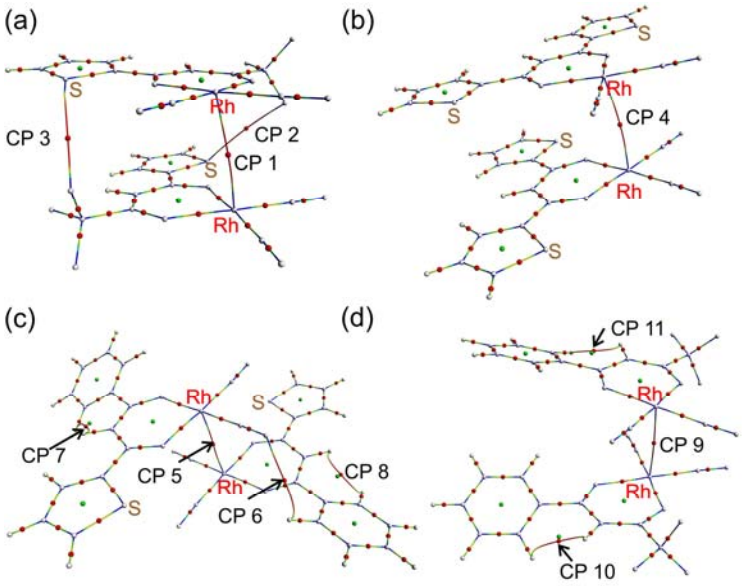

Figure 8. (a) Schematic representation of the critical points (CP) and bond paths (BP) for [Rh(R_1COCHCOR_2)(CO)$_2$], with R_1, R_2 = (a) CF_3, C_4H_3S (**1**), (b) C_4H_3S, C_4H_3S (**2**), (c) Ph, C_4H_3S (**3**) and (d) CF_3, Ph (**4**). The colour scheme identifying the critical points is as follows: white for (3, −3) or atom critical point; red for (3, −1) or bond CP; green for (3, +1) or ring CP. BPs colour scale is according to the value of the electron density: from blue/high to green to red/low.

4 Conclusion

A crystallographic study on a range of thienyl-containing [Rh(RCOCHCOC$_4$H$_3$S)(CO)$_2$] compounds (**1-3**), exhibiting dinuclear units, with experimentally measured Rh···Rh distances within each dinuclear unit, of 3.231 and 3.366 Å (R = CF_3), 3.190 Å (R = C_4H_3S) and 3.250 Å (R = Ph), was used to identify infinite approximately linear arrays of rhodium centers. The experimentally measured intermolecular Rh···Rh distances between the various dinuclear units are 3.622 and 3.412 Å (R = CF_3), 3.317 Å (R = C_4H_3S) and 3.250 Å (R = Ph). Further, a low temperature crystallographic study on a related non-thienyl-containing complex, [Rh(CF_3COCHCOPh)(CO)$_2$] (**4**), as well as its comparison with the literature ambient study, showed that the Rh···Rh metallophilic interactions of 3.529 Å in (**4**) are virtually temperature independent, and longer than observed for (**1**) - (**3**) or other related [Rh(β-diketonato)(CO)$_2$] complexes. Intermolecular halogen interactions in (**4**), connecting neighbouring molecules *via* the carbonyl moeity of (**4**) in a head-to-tail motif, futher stablize the linear arrays of rhodium centers in (**4**). Quantum-chemical calculations provide an electronic description of the intermolecular Rh···Rh interactions observed between the rhodium atoms in the dinuclear units of (**1**) - (**4**), by means of overlap of the non-bonding HOMOs of mainly d_{z2} character in different molecules of (**1**) - (**4**) with each other; to form bonding and non-bonding molecular orbitals in dinuclear units of (**1**) -

(**4**). NBO analyses indicate an LP(Rh1 d_{z2}) to LP*(Rh2 p_z) interaction between rhodium atoms from different [Rh(RCOCHCOC$_4$H$_3$S)(CO)$_2$] molecules within a dinuclear unit, while QTAIM analyses indicate a bonding path between rhodium atoms of different molecules within a dinuclear unit of (**1**) - (**4**).

Supporting Information

Crystallographic data has been deposited at the Cambridge Crystallographic Data Centre, with numbers: 1524292 (**1**), 1524293 (**2**) and 1543936 (**4**). Copies can be obtained, free of charge, on application to CCDC, 12 Union Road, Cambridge CB2 1EZ, UK [fax: +44 (0)1223 336033 or www.ccdc.cam.ac.uk/products/csd/request/]. Selected crystallographic, experimental and DFT data and the optimized coordinates of the DFT calculations, are given in the Supporting Information.

Acknowledgements

This work has received support from the South African National Research Foundation and the Central Research Fund of the University of the Free State, Bloemfontein, South Africa. The High Performance Computing facility of the UFS is acknowledged for computer time. AR and CP also gladly acknowledge support from SASOL.

References

[1] (a) M.-M. Rohmer, I. P.-C. Liu, J.-C. Lin, M.-J. Chiu, C.-H. Lee, G.-H. Lee, M. Bénard, X. López, S.-M. Peng, Structural, Magnetic, and Theoretical Characterization of a Heterometallic Polypyridylamide Complex, Angewandte Chemie, Int. Ed. 46 (2007) 3533–3536. DOI: 10.1002/anie.200604313
(b) J.F. Berry, Multiple Bonds between Metal Atoms, ed. F.A. Cotton, C.A. Murillo, R.A. Walton, Springer, New York, 3rd edn, 2005, ch.15, pp. 669–706.
[2] (a) V.W.-W. Yam, K.M.-C. Wong, N. Zhu, Solvent-Induced Aggregation through Metal···Metal/π···π Interactions: Large Solvatochromism of Luminescent Organoplatinum(II) Terpyridyl Complexes, Journal of the American Chemical Society 124 (2002) 6506–6507. DOI: 10.1021/ja025811c
(b) L.R. Falvello, J. Forniés, R. Garde, A. Garcia, E. Lalinde, M. T. Moreno, A. Steiner, M. Tomás, I. Usón, Tri-[Pt_2Tl]$^{3-}$ and Polynuclear Chain [Pt−Tl]$_\infty^-$ Complexes Based on Nonbridged Pt^{II}–Tl^{I} Bonds: Solid State and Frozen Solution Photophysical Properties, Inorganic Chemistry 45 (2006) 2543–2552. DOI: 10.1021/ic051818u
(c) W. Chen, F. Liu, D. Xu, K. Matsumoto, S. Kishi, M. Kato, Luminescent Amidate-Bridged One-Dimensional Platinum(II)−Thallium(I) Coordination Polymers Assembled via Metallophilic Attraction, Inorganic Chemistry 45 (2006) 5552–5560. DOI: 10.1021/ic051932c

(d) B. Liu, W. Chen, S. Jin, Synthesis, Structural Characterization, and Luminescence of New Silver Aggregates Containing Short Ag-Ag Contacts Stabilized by Functionalized Bis(*N*-heterocyclic carbene) Ligands, Organometallics 26 (2007) 3660–3667. DOI: 10.1021/om0701928
(e) E.J. Fernández, A. Laguna, J.M. López-de-Luzuriaga, Gold–heterometal complexes. Evolution of a new class of luminescent materials, Dalton Transactions (2007) 1969–1981. DOI: 10.1039/B702838P
(f) K. Jang, I.G. Jung, H.J. Nam, D.-Y. Jung, S.U. Son, One-Dimensional Organometallic Molecular Wires via Assembly of $Rh(CO)_2Cl$(amine): Chemical Control of Interchain Distances and Optical Properties, Journal of the American Chemical Society 131 (2009) 12046–12047. DOI: 10.1021/ja904247e
(g) R. Mas-Ballesté, R. González-Prieto, A. Guijarro, M.A. Fernández-Vindel, F. Zamora, Nanofibers generated by self-assembly on surfaces of bimetallic building blocks, Dalton Transactions (2009) 7341–7343. DOI: 10.1039/B911002J
[3] (a) M.-L. Kontkanen, L. Oresmaa, M.A. Moreno, J. Jänis, E. Laurila, M. Haukka, One-dimensional metal atom chain $[Ru(CO)_4]_n$ as a catalyst precursor — Hydroformylation of 1-hexene using carbon dioxide as a reactant, Applied Catalysis A 365 (2009) 130–134. DOI: http://dx.doi.org/10.1016/j.apcata.2009.06.006
(b) M.-N. Collomb-Dunand-Saunthier, A. Deronzier, R. Ziessel, Electrocatalytic Reduction of Carbon Dioxide with Mono(bipyridine)carbonylruthenium Complexes in Solution or as Polymeric Thin Films, Inorg. Chem. 33 (1994) 2961–2967. DOI: 10.1021/ic00091a040
(c) M.-N. Collomb-Dunand-Saunthier, A. Deronzier, R. Ziessel, Electrocatalytic reduction of CO_2 in water on a polymeric $[\{Ru^0(bpy)(CO)_2\}_n]$(bpy = 2,2′-bipyridine) complex immobilized on carbon electrodes, Journal of the Chemical Society, Chemical Communications (1994) 189–191. DOI: 10.1039/C39940000189
(d) L. Oresmaa, M.A. Moreno, M. Jakonen, S. Suvanto, M. Haukka, Catalytic activity of linear chain ruthenium carbonyl polymer $[Ru(CO)_4]_n$ in 1-hexene hydroformylation, Applied Catalysis A 353 (2009) 113–116. DOI: http://dx.doi.org/10.1016/j.apcata.2008.10.028
(e) M. Haumann, R. Meijboom, J.R. Moss, A. Roodt, Synthesis, crystal structure and hydroformylation activity of triphenylphosphite modified cobalt catalysts. Dalton Trans. (2004), 1679–1686, DOI: 10.1039/B403033H
(f) R. Crous, M. Datt, M. Foster, D. Bennie, L. Steenkamp, C. Huyser, J. Kirsten, L. Steyl, A. Roodt, Rhodium hydride formation in the presence of a bulky phosphite: spectroscopic and crystallographic study, Dalton Trans. (2005) 1108–1116, DOI: 10.1039/B416917D
(g) R. Meijboom, M. Haumann, A. Roodt, L. Damoense, Synthesis, spectroscopy and hydroformylation activity of sterically demanding phosphite-modified cobalt catalysts. Helvetica Chimica Acta (2005), 676-693, DOI: 10.1002/hlca.200590047
(h) A.C. Ferreira, R. Crous, L. Bennie, A. M. M. Meij, K. Blann, B. C. B. Bezuidenhoudt, D.A. Young, M. J. Green, A. Roodt, Borate Esters as Alternative Acid Promoters in the Palladium-Catalyzed Methoxycarbonylation of Ethylene. Angewandte Chemie International Edition 46, (2007), 2273-2275, DOI: 10.1002/anie.200603751
(i) A. Brink, A. Roodt, G. Steyl, H.G. Visser, Steric vs. electronic anomaly observed from iodomethane oxidative addition to tertiary phosphine modified rhodium(I) acetylacetonato complexes following progressive phenyl replacement by cyclohexyl [PR_3 = PPh_3, PPh_2Cy, $PPhCy_2$ and PCy_3], Dalton Trans. (2010) 5572-5578. DOI: 10.1039/B922083F
(j) N. Cloete, H.G. Visser, I. Engelbrecht, M. J. Overett, W. F. Gabrielli, A. Roodt, Ethylene Tri- and Tetramerization: A Steric Parameter Selectivity Switch from X-ray Crystallography and Computational Analysis, Inorg. *Chem.* 52 (2013) 2268-2270. DOI: 10.1021/ic302578a
[4] (a) J. Simon, J.J. Andre, Molecular Semiconductors, Springer, Berlin, 1985.
(b) W. Lu, V.A.L. Roy, C.-M. Che, Self-assembled nanostructures with tridentate cyclometalated platinum(II) complexes, Chemical Communications (2006) 3972–3974. DOI: 10.1039/B607422G

(c) C. Femoni, F. Kaswalder, M.C. Iapalucci, G. Longoni, S. Zacchini, Infinite Molecular $\{[Pt_{3n}(CO)_{6n}]^{2-}\}_{\infty}$ Conductor Wires by Self-Assembly of $[Pt_{3n}(CO)_{6n}]^{2-}$ (n = 5–8) Cluster Dianions Formally Resembling CO-Sheathed Three-Platinum Cables, European Journal of Inorganic Chemistry (2007) 1483–1486. DOI: 10.1002/ejic.200700097
(d) A. Guijarro, O. Castillo, A. Calzolari, P.J. Sanz Miguel, C.J. Gómez-García, R. di Felice, F. Zamora, Electrical Conductivity in Platinum-Dimer Columns, Inorganic Chemistry 47 (2008) 9736–9738. DOI: 10.1021/ic801211m
(e) S. Myllynen, M. Wasberg, High electrical conductivity for the partially oxidised d8 Ru-Ru bonded chain [Ru(bpy)(CO)2]n (bpy = 2,2'-bipyridine) and its wide range redox control, Electrochemistry Communications 11 (2009) 1453–1456. DOI: http://dx.doi.org/10.1016/j.elecom.2009.05.029
(f) G. Givaja, P. Amo-Ochoa, C.J. Gómez-Garcìa, F. Zamora, Electrical conductive coordination polymers, Chemical Society Review 41 (2012) 115–147. DOI: 10.1039/C1CS15092H
[5] (a) Swager, T. The molecular wire approach to sensory signal amplification. Accounts of Chemical Research 31 (1998) 201–207. DOI: 10.1021/ar9600502
(b) R.L. Carroll, C.B. Gorman, The genesis of molecular electronics, Angewandte Chemie, Int. Ed. 41 (2002) 4378–4400. DOI: 10.1002/1521-3773(20021202)41:23<4378::AID-ANIE4378>3.0.CO;2-A
(c) M.J. Frampton, H.L. Anderson, Insulated molecular wires, Angewandte Chemie, Int. Ed. 46 (2007) 1028–1064. DOI: 10.1002/anie.200601780
(d) Cheng, Y-J., Yang, S-H. & Hsu, C-S. Synthesis of conjugated polymers for organic solar cell applications. Chem. Rev. 109 (2009) 5868–5923. DOI: 10.1021/cr900182s
(e) S.E. Habas, H.A.A. Platt, M.F.A.M. van Hest, D.S. Ginley, Low-Cost Inorganic Solar Cells: From Ink To Printed Device, Chemical Reviews 110 (2010) 6571–6594. DOI: 10.1021/cr100191d
[6] M. Jakonen, L. Oresmaa, M. Haukka, Solid-State Packing of the Square-Planar $[Rh^{I}(H_2bim)(CO)_2]_2[A]$ Complexes (H_2bim = 2,2-biimidazole; [A] = 2[Cl], 2[$Rh^{I}Cl_2(CO)_2$], [$Fe^{II}Cl_4$], [$Co^{II}Cl_4$]), Crystal Growth & Design 7 (2007) 2620-2626. DOI: 10.1021/cg070577t
[7] (a) J.S. Miller, Extended linear chain compounds, Plenum Press: New York, 1982, Vol. 1–3.
(b) J.K. Bera, K.R. Dunbar, Chain Compounds Based on Transition Metal Backbones: New Life for an Old Topic, Angewandte Chemie, Int. Ed. 41 (2002) 4453-4457. DOI: 10.1002/1521-3773
[8] J. Conradie, A comparative DFT study of stacking interactions between adjacent metal atoms in linear chains of Ir and Rh acetylacetonato complexes, Journal of Organometallic Chemistry, 833 (2017) 88-94. DOI: 10.1016/j.jorganchem.2017.01.032
[9] M.M. Conradie, J. Conradie, Solid state packing of [Rh(β-diketonato)$(CO)_2$] complexes. Crystal structure of [Rh(PhCOCHCOC$_4H_3S$)$(CO)_2$], Journal of Molecular Structure 1051 (2013) 137-143. DOI: 10.1016/j.molstruc.2013.07.046
[10] J. Conradie, Stacking of dicarbonylacetylacetonatorhodium(I) molecules, Computational and Theoretical Chemistry, 2017, online, DOI: 10.1016/j.comptc.2016.12.024
[11] J.G. Leipoldt, L.D.C. Bok, S.S. Basson, J.S. van Vollenhoven, T.I.A. Gerber, The crystal structure of benzoyl-1,1,1-trifluoroacetonatodicarbonylrhodium(I), Inorganica Chimica Acta 25 (1977) L63-L64. DOI: 10.1016/S0020-1693(00)95646-9
[12] (a) M.M. Conradie, J. Conradie, A Kinetic Study of the Oxidative Addition of Methyl Iodide to [Rh((C$_4H_3S$)COCHCOCF_3)(CO)(PPh_3)] utilizing UV/vis and IR Spectrophotometry and ^{1}H, ^{19}F and ^{31}P NMR Spectroscopy. Synthesis of [Rh((C$_4H_3S$)COCHCOCF_3)(CO)(PPh_3)(CH_3)(I)] Inorganica Chimica Acta 361 (2008) 208-218. DOI: 10.1016/j.ica.2007.07.010
(b) M.M. Conradie, J. Conradie, Methyl Iodide Oxidative Addition to Monocarbonylphosphine [Rh((C$_4H_3S$)COCHCOR)(CO)(PPh_3)] Complexes Utilizing UV/vis and IR Spectrophotometry and NMR Spectroscopy to Identify Reaction Intermediates. R = C_6H_5 or C_4H_3S, Inorganica Chimica Acta 361 (2008) 2285-2295. DOI: 10.1016/j.ica.2007.10.052

[13] (a) P. Serp, M. Hernandez, B. Richard, P. Kalck, A Facile Route to Carbonylhalogenometal Complexes (M = Rh, Ir, Ru, Pt) by Dimethylformamide Decarbonylation, European Journal of Inorganic Chemistry 9 (2001) 2327-2336. DOI: 10.1002/1099-0682(200109)2001:9<2327::AID-EJIC2327>3.0.CO;2-D
(b) Y.S. Varshavsky, T.G. Cherkasova, Remarks on the process of homogeneous carbonylation of rhodium compounds by N,N-dimethylformamide, J. Organomet. Chem. 692 (2007) 887-893. DOI: 10.1016/j.jorganchem.2006.10.040
[14] M.M. Conradie, A.J. Muller, J. Conradie, Thienyl-containing β-diketones: synthesis, characterization, crystal structure, keto-enol kinetics, S. Afr. J. Chem. 61 (2008) 13-21. http://www.journals.co.za/sajchem/
[15] APEX2 (including SAINT and SADABS); Bruker AXS Inc., Madison, WI, 2012.
[16] G. M. Sheldrick, A short history of SHELX, Acta Cryst. A64 (2008) 112-122. DOI: 10.1107/S0108767307043930
[17] L.J. Farrugia, WinGX and ORTEP for Windows: an update, J. Appl. Cryst. 45 (2012) 849–854. DOI:10.1107/S0021889812029111
[18] J.P. Perdew, J.A. Chevary, S.H. Vosko, K.A. Jackson, M.R. Pederson, D.J. Singh, C. Fiolhais, Atoms, molecules, solids, and surfaces: Applications of the generalized gradient approximation for exchange and correlation, Physical Review B 46 (1992) 6671-6687. Erratum: J.P. Perdew, J.A. Chevary, S.H. Vosko, K.A. Jackson, M.R. Perderson, D.J. Singh, C. Fiolhais, Physical Review B 48 (1993) 4978. DOI: 10.1103/PhysRevB.46.6671
[19] B. Miehlich, A. Savin, H. Stoll, H. Preuss, Results obtained with the correlation-energy density functionals of Becke and Lee, Yang and Parr, Chem. Phys. Lett. 157 (1989) 200-06. DOI: 10.1016/0009-2614(89)87234-3.
[20] H. Iikura, T. Tsuneda, T. Yanai, and K. Hirao, Long-range correction scheme for generalized-gradient-approximation exchange functionals, J. Chem. Phys. 115 (2001) 3540-44. DOI: 10.1063/1.1383587
[21] A.D. Becke, Density-functional exchange-energy approximation with correct asymptotic behavior, Physical Review A 38 (1988) 3098–3100. DOI: 10.1103/PhysRevA.38.3098
[22] C.T. Lee, W.T. Yang, R.G. Parr, Development of the Colle-Salvetti correlation-energy formula into a functional of the electron density, Physical Review B 37 (1988) 785–789. DOI 10.1103/PhysRevB.37.785
[23] T. Yanai, D. Tew, N. Handy, A new hybrid exchange-correlation functional using the Coulomb-attenuating method (CAM-B3LYP), Chem. Phys. Lett. 393 (2004) 51-57. DOI: 10.1016/j.cplett.2004.06.011.
[24] Grimme, S.; Antony, J.; Ehrlich, S.; Krieg, H.; A consistent and accurate ab initio parametrization of density functional dispersion correction (DFT-D) for the 94 elements H-Pu. J. Chem. Phys. 132, (2010), 154104. doi.org/10.1063/1.3382344
[25] Y. Zhao, D.G. Truhlar, The M06 suite of density functionals for main group thermochemistry, thermochemical kinetics, noncovalent interactions, excited states, and transition elements: two new functionals and systematic testing of four M06-class functionals and 12 other functionals, Theor. Chem. Acc. 120 (2008) 215-41. DOI: 10.1007/s00214-007-0310-x
[26] S. Grimme, J. Antony, S. Ehrlich, H. Krieg, A consistent and accurate ab initio parametrization of density functional dispersion correction (DFT-D) for the 94 elements H-Pu. J. Chem. Phys. 132 (2010) 154104. doi.org/10.1063/1.3382344
[27] M.J. Frisch, G.W. Trucks, H.B. Schlegel, G.E. Scuseria, M.A. Robb, J.R. Cheeseman, G. Scalmani, V. Barone, B. Mennucci, G.A. Petersson, H. Nakatsuji, M. Caricato, X. Li, H.P. Hratchian, A.F. Izmaylov, J. Bloino, G. Zheng, J.L. Sonnenberg, M. Hada, M. Ehara, K. Toyota, R. Fukuda, J. Hasegawa, M. Ishida, T. Nakajima, Y. Honda, O. Kitao, H. Nakai, T. Vreven, J.A. Montgomery (Jr), J.E. Peralta, F. Ogliaro, M. Bearpark, J.J. Heyd, E. Brothers, K.N. Kudin, V.N. Staroverov, T. Keith, R. Kobayashi, J. Normand, K. Raghavachari, A. Rendell, J.C. Burant, S.S.

Iyengar, J. Tomasi, M. Cossi, N. Rega, J.M. Millam, M. Klene, J.E. Knox, J.B. Cross, V. Bakken, C. Adamo, J. Jaramillo, R. Gomperts, R.E. Stratmann, O. Yazyev, A.J. Austin, R. Cammi, C. Pomelli, J.W. Ochterski, R.L. Martin, K. Morokuma, V.G. Zakrzewski, G.A. Voth, P. Salvador, J.J. Dannenberg, S. Dapprich, A.D. Daniels, O. Farkas, J.B. Foresman, J.V. Ortiz, J. Cioslowski, D.J. Fox, Gaussian 09, Revision D.01, Gaussian Inc., Wallingford CT, 2010.
[28] (a) T.H. Dunning Jr., P.J. Hay, in: H.F. Schaefer (Ed.), Modern Theoretical Chemistry, Vol. 3, Plenum, New York, 1976, pp. 1-28.
(b) P.J. Hay, W.R. Wadt, *Ab initio* effective core potentials for molecular calculations. Potentials for the transition metal atoms Sc to Hg, Journal of Chemical Physics 82 (1985) 270–283. DOI 10.1063/1.448799
(c) P.J. Hay, W.R. Wadt, *Ab initio* effective core potentials for molecular calculations. Potentials for main group elements Na to Bi, Journal of Chemical Physics 82 (1985) 284–298. DOI 10.1063/1.448800
(d) P.J. Hay, W.R. Wadt, *Ab initio* effective core potentials for molecular calculations. Potentials for K to Au including the outermost core orbitals, Journal of Chemical Physics 82 (1985) 299–310. DOI 10.1063/1.448975
[29] E.D. Glendening, J.K. Badenhoop, A.E. Reed, J.E. Carpenter, J.A. Bohmann, C.M. Morales, F. Weinhold, NBO 3.1, Theoretical Chemistry Institute, University of Wisconsin, Madison, WI, USA, 2001.
[30] (a) R.F.W. Bader, A quantum theory of molecular structure and its applications, Chemical Reviews 91 (1991) 893–928. DOI: 10.1021/cr00005a013
(b) F. Cortés-Guzmán, R.F.W. Bader, Complementarity of QTAIM and MO theory in the study of bonding in donor–acceptor complexes, Coordination Chemistry Reviews 249 (2005) 633–633. doi:10.1016/j.ccr.2004.08.022
[31] J.I. Rodríguez, R.F.W. Bader, P.W. Ayers, C. Michel, A.W. Götz, C. Bo, A high performance grid-based algorithm for computing QTAIM properties, Chemical Physics Letters 472 (2009) 149–152. DOI 10.1016/j.cplett.2009.02.081
[32] (a). G. te Velde, F.M. Bickelhaupt, S.J.A. van Gisbergen, C.F. Guerra, E.J. Baerends, J.G. Snijders, T. Ziegler, Chemistry with ADF, Journal of Computational Chemistry 22 (2001) 931–967. DOI: 10.1002/jcc.1056
(b) C.F. Guerra, J.G. Snijders, G. te Velde, E.J. Baerends, Towards an order-N DFT method, Theoretical Chemistry Accounts 99 (1998) 391–403. DOI 10.1007/s002140050353
(c) ADF2013, SCM, Theoretical Chemistry, Vrije Universiteit, Amsterdam, The Netherlands, 2013. http://www.scm.com
[33]O.V. Sizova, Y.S. Varshavskii, A.B. Nikol'skii, Binuclear Rhodium(I) Carbonyl Carboxylate Complexes: DFT Study of Structural and Spectral Properties, Russian Journal of Coordination Chemistry 31 (2005) 875–883. DOI: 10.1007/s11173-005-0185-0
[34] K.H. Hopmann, J. Conradie, A Density Functional Theory Study of Substitution at the Square-Planar Acetylacetonato-dicarbonyl-rhodium(I) complex, Organometallics 28 (2009) 3710–3715. DOI: 10.1021/om900133s
[35] K.H. Hopmann, N.F. Stuurman, A. Muller, J. Conradie, Substitution and Isomerisation of Asymmetric β-Diketonato Rhodium (I) Complexes: A Crystallographic and Computational Study, Organometallics 29 (2010) 2446–2458. DOI: 10.1021/om1000138
[36] L.J. Farrugia, WinGX and ORTEP for Windows: an update, Journal of Applied Crystallography 45 (2012) 849-854. DOI: 10.1107/S0021889812029111
[37] Y. Ohashi, C.W. Burnham, Clinopyroxene lattice deformations: The roles of chemical substitution and temperature, American Mineralogist 58 (1973) 843-849.
[38] P. Müller, Practical suggestions for better crystal structures, Crystallography Reviews 15 (2009) 57-83. DOI: 10.1080/08893110802547240

[39] J.P.M. Lommerse, A.J. Stone, R. Taylor, F.H. Allen, The Nature and Geometry of Intermolecular Interactions between Halogens and Oxygen or Nitrogen, J. Am. Chem. Soc. 118 (1996) 3108-3116. DOI: 10.1021/ja953281x
[40] P. Metrangola, J. S. Murray, T. Pilati, P. Politzer, G. Resnatti, G. Terraneo, Fluorine-Centered Halogen Bonding: A Factor in Recognition Phenomena and Reactivity, Cryst. Growth Des. 11 (2011) 4238-4246. DOI: 10.1021/cg200888n
[41] N.F. Stuurman, R, Meijboom, J. Conradie, Characterization of [Rh(PhCOCHCOCH$_2$CH$_2$CH$_3$)(CO)$_2$] by X-ray Crystallography, a Computational and a Statistical Study, Polyhedron 30 (2011) 660-665. DOI: 10.1016/j.poly.2010.11.038
[42] J. Conradie, T.S. Cameron, M.A.S. Aquino, G.J. Lambrecht, J.C. Swarts, Synthetic, electrochemical and structural aspects of a series of ferrocene-containing dicarbonyl betadiketonato rhodium(I) complexes, Inorganica Chimica Acta 358 (2005) 2530-2542. DOI:10.1016/j.ica.2005.02.010
[43] C. Pretorius, A. Brink, A. Roodt, Crystal structure of acetopyruvato-κ^2 O,O-dicarbonylrhodium(I), $C_8H_7O_6Rh$. Zeitschrift fur Krystallographie: New Crystal Structures 229 (2014). 371-372. DOI: 10.1515/ncrs-2014-0195
[44] F. Huq, A.C. Skapski, Refinement of the crystal structure of acetylacetonatodicarbonylrhodium(I), Journal of Crystal and Molecular Structure 4 (1974) 411-418. DOI: 10.1007/BF01220097
[45] C. Pretorius, A. Roodt, (Benzoyl-acetonato-κ^2O,O')dicarbonyl-rhodium(I), Acta Crystallographica E68 (2012) m1451-m1452. DOI: 10.1107/S1600536812044893
[46] W.J. Hehre, A Guide to Molecular Mechanisms and Quantum Chemical Calculations, Wavefunction Inc., Irvine, CA, USA, 2003, pp. 153,181.
[47] (a) M.M. Conradie, J. Conradie, Methyl Iodide Oxidative Addition to Rhodium(I) Complexes: a DFT and NMR Study of [Rh(FcCOCHCOCF$_3$)(CO)(PPh$_3$)] and the Rhodium(III) Reaction Products, South African Journal of Chemistry 61 (2008) 102-111. (b) M.M. Conradie, J. Conradie, Stereochemistry of the Reaction Products of the Oxidative Addition Reaction of Methyl Iodide to [Rh((C$_4$H$_3$S)COCHCOR)(CO)(PPh$_3$)]: a NMR and Computational Study. R = CF$_3$, C$_6$H$_5$, C$_4$H$_3$S, Inorganica Chimica Acta 362 (2009) 519-530. DOI: 10.1016/j.ica.2008.04.046. (c) M.M. Conradie, J. Conradie, A Density Functional Theory Study of the Oxidative Addition of Methyl Iodide to Square Planar [Rh(acac)(P(OPh)$_3$)$_2$] complex and simplified model systems, J Organomet. Chem. 695 (2010) 2126-2133. DOI:10.1016/j.jorganchem.2010.05.021. (d) J. Conradie, Density Functional Theory Calculations of Rh-β-diketonato complexes, Journal of the Chemical Society, Dalton Transactions 44 (2015) 1503–1515. DOI:10.1039/C4DT02268H
[48] R.F.W. Bader, A Bond Path: A Universal Indicator of Bonded Interactions, Journal of Physical Chemistry A 102 (1998) 7314-7323. DOI: 10.1021/jp981794v